INSTITUTO DE ENGENHARIA NUCLEAR

RT-IEN- 12/2002

A hybrid technique to evaluate the Line Spread Function

por

Gevaldo L. de Almeida, Maria Inês Silvani Souza, Ricardo Tadeu Lopes

Junho/2002

INSTITUTO DE ENGENHARIA NUCLEAR

Título: A hybrid technique to evaluate the Line Spread Function

Autor (es): Gevaldo L. de Almeida
Maria Ines Silvani Souza
Ricardo Tadeu Lopes

e-mail: gevaldo@ien.gov.br
msouza@ien.gov.br

Identificação: RT-IEN-12/2002	Nº de páginas: 12	Tipo de Divulgação: Irrestrita (x) Restrita ( )	Divulgar para: IEN	Localização: INTRANET

Publicação externa associada (congresso/periódico): VI ENAN INAC 2002

Palavras chave: line spread function, edge response function, tomography, image quality

Resumo: A hybrid technique to evaluate the *Line Spread Function (LSF)* has been developed. It's based on an experimental-theoretical approach aiming the reduction of the required experimental efforts to reach an acceptable level of accuracy on the width of the Gaussian representing the LSF. Using this technique, the several spectra required to fill up the space domain with an adequate density, usually done by shifting slightly the object with respect to the source-detector system after each spectrum is taken, are replaced by few spectra and a theoretical treatment involving numerical integration and non-linear fittings. In order to accomplish this task, a function is fitted to the experimental data, allowing the accurate determination of the center of the cylindrical object in the spectrum. Once this center is determined, it becomes possible to compare channel by channel the experimental counts with the expected theoretical ones. The first ones represent an integration of the transmitted neutron beam, as automatically performed by the detector, and hence, to achieve the aimed comparison, the theoretical counts should as well arise from a similar integration. Since the function expressing the transmitted beam intensity cannot be symbolically integrated, the task is done numerically over regular intervals corresponding to each given nominal collimator aperture. The sum of quadratic differences between the experimental and calculated counts reaches a minimum at an *effective collimator aperture*, which is somewhat different from the *nominal aperture* actually used in the experiments due to the unavoidable neutron scattering process and statistical fluctuations. This effective aperture is then used to get through integration the theoretical *Edge Response Function (ERF)* spectrum for any displacement step. Such a feature makes possible the simulation of high density spectra which are otherwise experimentally unfeasible due to the limited mechanical tolerances of the positioning devices. A derivation of the ERF yields the aimed LSF. Several comparisons and simulations have then be made by using a computer program written in Fortran, to evaluate the applicability and advantages of the developed technique.

Emissão		Nome	Rubrica	Data
Data:	Elaboração:	Gevaldo L. de Almeida, Maria Ines S. Souza, Ricardo Tadeu Lopes		
Divisão: DIRE	Revisão:	Carlos Alberto Renke		
Serviço: SEREA	Aprovação :	Orlando Agostinho		

Instituto de Engenharia Nuclear:
Via 5 s/n, Cidade Universitária, Ilha do Fundão, CEP 21945-970, CP 68.550, Rio de Janeiro – RJ - Brasil .
Tel.: 00 55 21 2560-4113 Internet: www.ien.gov.br

A HYBRID TECHNIQUE TO EVALUATE THE LINE SPREAD FUNCTION

Gevaldo L. de Almeida*, Maria Ines S. Souza*, Ricardo T. Lopes**

*Instituto de Engenharia Nuclear – IEN-CNEN/RJ
Caixa Postal 68550
21945-970, Rio de Janeiro, Brasil

**Laboratório de Instrumentação Nuclear – COPPE/UFRJ
Caixa Postal 68509
21945-970, Rio de Janeiro, Brasil

I. INTRODUCTION

One of the most useful tools to evaluate on a quantitative basis the performance of an image acquiring system is the *Modulation Transfer Function-MTF*. This function expresses how the ability of the system to distinguish single close features is impaired by decreasing the distance between them. The MTF can be obtained by the discrete Fourier Transformation of the *Line Spread Function-LSF* [1]. An equivalent function used to evaluate a system is the *Contrast Response* curve which can be experimentally obtained by using a special collimator provided with constant aperture slits but with increasing spatial frequency. Due to its high cost, the former curve is usually a better alternative, which requires nevertheless the knowledge of the LSF.

This function is a measure of the spatial resolution for a given image acquiring system, being expressed by a curve of the fraction of radiation registered versus the distance along a line perpendicular to the radiation beam, whenever a line source perpendicular to both is *examined* by that system.

Rather than a thin line, a more or less blurred image is obtained depending on the spatial resolution for that particular system. A simple method to obtain a good approximation of the LSF is through differentiation of the *Edge Response Function-ERF*, experimentally obtained by measuring the intensity of a thin radiation beam gradually intercepted by an opaque cylinder. Usually, several ERF profiles are measured and averaged to improve the statistics. In this work a hybrid technique has been developed to obtain the LSF. Rather than taking several ERF spectra, a theoretical function is fitted to some of them, sparing thus time and experimental effort. After differentiation of that function, a Gaussian curve is fitted to the result, making thus possible to assign a FWHM, characterizing thus the spatial resolution of the system, as well as to apply the discrete Fourier Transformation to that Gaussian to obtain the *Modulation Transfer Function.*

II. THEORETICAL APPROACH

Basic Principles. A set of aligned single features - like dots for instance - where the gap between two consecutive of them decreases continuously, would produce a linear image where at first the dots could be recognized as individual entities, but as the gap gradually diminishes, it becomes more and more difficult until the utter impossibility to do that, when that part of the image is reduced to a blurred strip.

If some kind of variable is assigned to the dots and gaps - 0 for dots and 1 for gaps for instance - the image could be represented by an oscillatory function of increasing spatial frequency. The higher this frequency, the greater the *invasion* of the pure gap regions by the penumbra surrounding the dots, i.e., the intensity at the gaps would no longer be 1 but a lower value decreasing with the frequency, until zero. Hence, the *amplitude* of that oscillatory function would be *modulated* by the specific ability of the system to resolve close features.

An alternative way to get a similar curve to the MTF - the *Contrast Response* curve - is through the using of a multi-slit collimator made of a blade of opaque material to the utilized radiation. Such collimators are expensive and therefore other methods have been conceived to bypass this handicap. One of these methods is the discrete Fourier Transformation of the *Line Spread Function-LSF.*

Whenever a line source is *examined* by a given acquiring system, rather than a thin line, a more or less blurred image is obtained depending on its resolution power. The curve expressing the fraction of radiation registered by the system versus the distance along a line perpendicular to the radiation beam is called the *Line Spread Function - LSF* for that particular system.

In the case of a X-ray or neutron tomographic system operating by transmission, a slit collimator simulates approximately a line source, whose intensity is modulated by the internal features of the object being scanned. Therefore, for each position in the scanning process there's an associated LSF with their maxima determined by the attenuation properties of the body under analysis along the beam path. Such a LSF could be experimentally determined by keeping the *source*, i.e., the slit collimator, and sample at a fixed position while a movable detector provided with a very narrow - compared to the LSF width - collimator aperture would scan the LSF domain.

This approach would require a modification of the tomographic system designed to keep the detector unmovable and aligned with the source. Moreover, due to the narrow aperture of the collimator attached to the detector, the counting time should be lenghtened to assure an acceptable statistics. These difficulties can be overcome at once, by keeping the system unchanged and performing an *integration* of the LSF over variable limits. This integration automatically carried out by the detector, improves the statistics.

For an unperturbed beam, i.e., no object between source and detector, the integration would be done over all the LSF domain, but if an opaque sample is placed between them, it would cut part of the beam, it means part of the LSF curve, changing thus one of the integration limits. Therefore, as the sample gradually *eclipses* the source, the count registered by the detector represents an integral of the remaining domain of the LSF. A plot of these counts against the position of the eclipsing sample is known as *Edge Response Function-ERF.* The original LSF can then be recovered by the differentiation of the ERF.

Since the position of the sample defines an integration limit, it should cut off completely any beam residue beyond that limit. This would be fulfilled only if the sample had a flat face perfectly parallel to the beam *and* an attenuation factor large enough to preclude any significant count at the *shadow zone*. It would be very difficult to fulfill the first condition - utilizing a prism for instance - because the beam could hit a corner first.

Hence, in practice, a cylinder is used as sample because it's always possible a tangential touch between a beam coming from any direction and the cylindrical surface. The using of a cylinder means nevertheless that the transmitted beam will not drop suddenly to zero, even for an infinitely thin beam, unless it had a huge radius, and therefore a compromise has to be done.

So, the LSF deduced from an ERF determined after this approach is only a good approximation. Taking into account that the counts are expected to drop quickly near the cylinder edge, it's necessary to choose a small translation step in order to obtain an ERF with an adequate density of points. An usual alternative way to do that is to acquire many ERF profiles and average them, reducing so the statistical uncertainty and the effect of the discrete displacement.

Algorithm. The intensity of a transmitted neutron beam emerging from an object bombarded by a mono-energetic ideally narrow neutron beam decays exponentially with the product of the macroscopic cross section times the traveled distance inside that object.

For an actual broad beam, such a simple equation no longer express the reality, specially when the shape of the object forces the beam to travel a variable thickness inside it. When a beam of flux intensity I_0 strikes a cylindrical body as those used to determine the *Line Spread Function* the average flux *Ia* of the transmitted beam can be expressed as:

$$I_a = \frac{I_0}{(x_2 - x_1)} \int_{x_1}^{x_2} e^{-\Sigma_{th} 2.\sqrt{R^2 - x^2}} dx \qquad x_1 > -R \qquad x_2 < R \qquad (1)$$

$$I_a = \frac{I_0}{(x_2 - x_1)} \int_{x_1}^{x_2} dx \qquad x_1 \leq -R \qquad x_2 \geq R \qquad (1a)$$

with the cylinder radius R aligned along the x-axis and the beam coming along the y-axis. The limits of integration x_1 and x_2 define the edges of the beam while Σth defines the neutron thermal cross section of the cylinder. The integrations (1) and (1a) are automatically performed by a detector placed behind the cylinder, and therefore allowing the uncertainties arising from the statistical fluctuations, the ratio I/I_0 should be the same within any integration interval for both theoretical and experimental processes.

Therefore, a fit of the system (1-1a) to the experimental data would produce a function capable to describe those data for any aimed cylinder displacement, a task which would experimentally difficult or even unfeasible due to the required mechanical precision for the positioning table.

This approach has three main advantages:

- It uses the whole experimental data set to produce a single symmetric curve with regard to the y-axis containing the center of the cylinder. Due to this symmetry, its derivative is anti-symmetric with regard to the same axis, and thus, the gaussians fitted to their tails have the same FWHM, as should be expected.
- The capability to get the I/I_0 ratio for any cylinder displacement means that the theoretical curve and its derivative can be represented by any desired density of points, allowing a more accurate determination of the gaussian FWHM.
- It forecasts the theoretical gaussian FWHM for any specified collimator aperture, serving therefore as a guide to plan the experiments to measure the actual FWHM.

Prior to fit the system (1-1a) to the experimental data, a variable transform should be carried out, for their x-axis have different off-sets. Indeed, for system (1-1a), the cylinder is centered at the x-axis origin, while for the experimental assembly it's located somewhere along the channel number scale.

Since the fitting process requires the knowledge of theoretical and experimental I/I_0 ratios at the very same x, the above mentioned off-set should be determined. To accomplish this task, a function is fitted to an experimental spectrum as follows:

$$T = T_0 . e^{-\Sigma_{th} .2\sqrt{R^2 - (x+D)^2}} \qquad -R < x < R \tag{2}$$

where T and T_0 are the count rates produced by the detector due to the fluxes I and I_0 respectively, and D is the approximate unknown off-set. It's only an approximate value because the Eq.(2) is itself an approximation too, being exact only for an infinitely narrow collimator aperture. This D-value will be later on used as starting point to get a more refined value. In this fitting process using the non-linear option of *Microcal Origin*, T_0 is set free to improve its accuracy.

After this approach, T_0 is determined using the set of T-values emerging from the cylinder, rather than taking the unperturbed T_0-values at both spectrum tails, which can be affected by poor beam alignment. Once D and T_0 are determined, the theoretical count-rate T_i at the ith-channel for a given collimator aperture w is evaluated by using the expressions as follows:

$$T_i = \frac{T_0}{w} \int_{x_i - \frac{w}{2}}^{x_i + \frac{w}{2}} e^{-\Sigma_{th} 2.\sqrt{R^2 - (x+D)^2}} dx \tag{3}$$

$$x_i = c_i - D \tag{3a}$$

where x_i is the position of channel c_i after a scale centered at the cylinder axis. A family of curves arising from equation (3) for several collimator apertures w, shown on Fig.1 present the expected features.

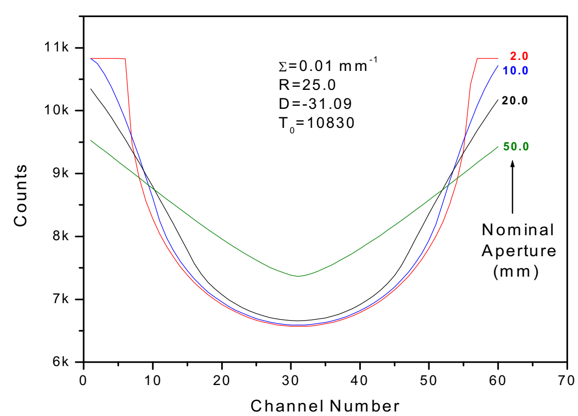

Figure 1. Family of curves for several collimator apertures after equation (3). The minimum value for each curve increases with w due to the contribution of higher neighbor counts around the central channel.

For n points, the sum of quadratic differences, between the counts for two given curves, one generated with a reference collimator aperture *wref* and the other with a generic aperture w_k

$$S(k) = \sum_{i=1}^{n} \left[T_i(w_k) - T_i(wref) \right]^2 \tag{4}$$

should reach *zero* when they assume the same *w*-value because otherwise the average fluxes and consequently the count rates wouldn't match. This can be observed in Fig.2, where that sum have been plotted against a variable w_k for a *wref*=2.

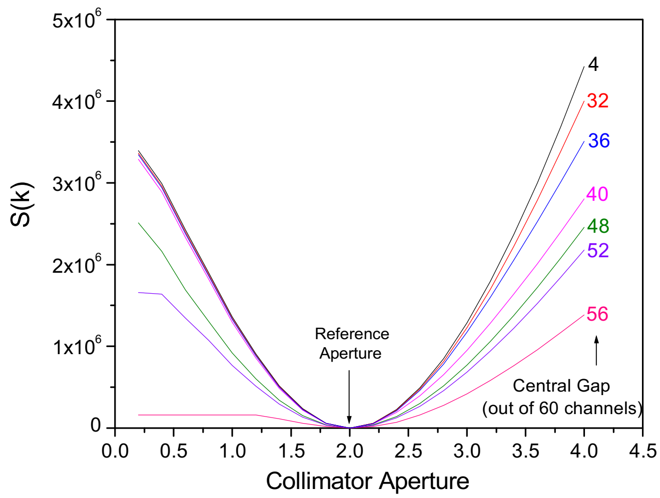

Figure 2. Behavior of S(k) for theoretical counts not affected by statistical fluctuations. It reaches *zero* when the *nominal aperture* w_k becomes equal to the *reference aperture wref*.

The central regions of the curves displayed in Fig. 1, are relatively flat, and therefore a variation in the collimator aperture shouldn't affect substantially S(k). To quantify this effect, S(k) has been assessed by leaving a variable gap around the central part of those curves. As observed on Fig. 2, only large gaps or large differences between w_k and *wref* have a substantial effect on S(k).

When $T_i(wref)$ are replaced by experimental data, *S(k)* no longer reaches zero, when $w_k=wref$ but a certain minimum value dictated by the statistical uncertainties. Moreover, the formerly determined approximate D-value should be refined by the experimental data themselves. For this purpose, S(k) is replaced by

$$S(m,k) = \sum_{i=1}^{n} \left[T_i(d_m, w_k) - T_i(wref) \right]^2 \tag{5}$$

where $Ti(d_m,w_k)$ is the theoretical count for a collimator aperture w_k and an off-set d_m. The minimal value of S(m,k) for a *dm* range around *D* and a *wk* range around *wref* furnishes the best fit for *D* and *w*.

As shown in Fig.3, this minimum is not so sharply defined as in previous case but nevertheless still very well visible due to the curve smoothness. As for the theoretical S(k) values shown on Fig. 2, the central gap do not affect the position of the curve minima.

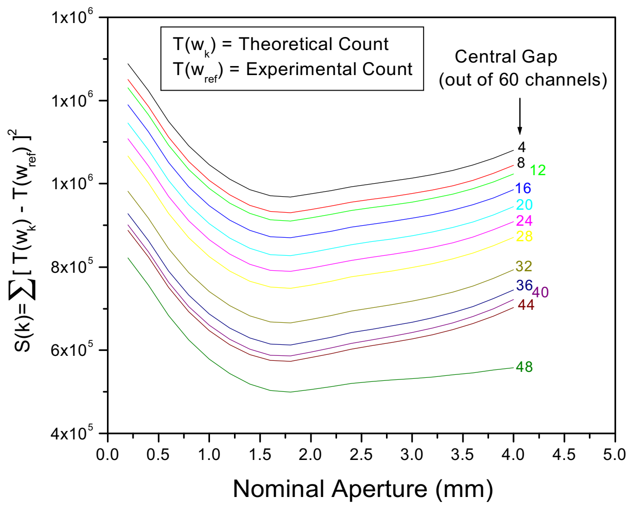

Figure 3. Behavior of S(k) for an actual experimental spectrum acquired using a 2 mm collimator. A minimum occurs at an *effective aperture* – w_{eff} of about 1.8 mm.

The value of w_k at where this minimum occurs corresponds to an *effective aperture*, i.e., the collimator aperture producing a curve generated by Eq.(3), best fitted to the experimental data. An example of both is shown in Fig. 4.

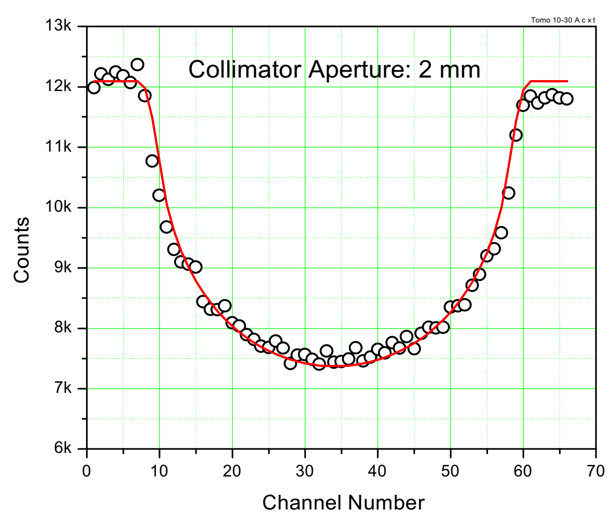

Figure 4. Example of an experimental spectrum and the best fit curve generated by the expressions (3-3a).

Each tail of the fitted curve represent an *Edge Response Functions-ERF* and their first derivatives can be used as a fair approximation of the *Line Spread Function* after a proper Gaussian fitting as shown on Fig.5.

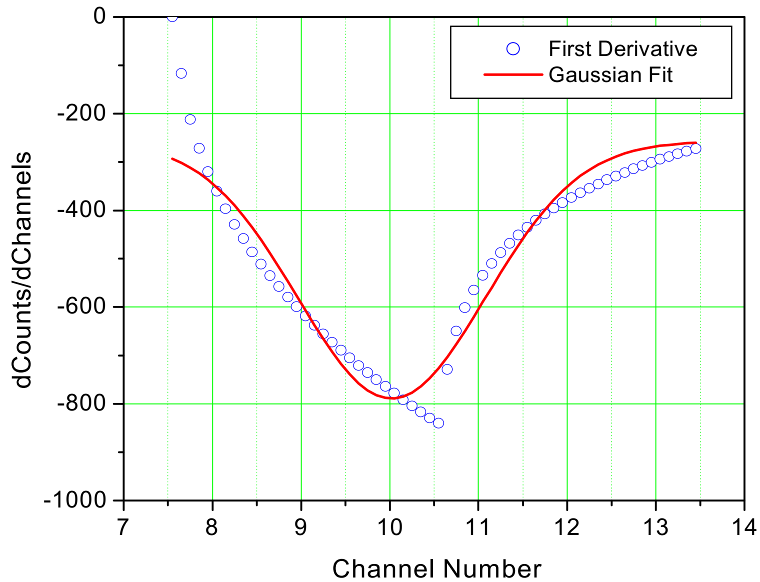

Figure 5. *Line Spread Function* and a Gaussian fitted to it. The rough data have been obtained by a numerical differentiation of the *Edge Response Function.*

In spite of the apparent disagreement between the rough data and the fitted curve, it should be stressed that the relevant parameter in this case is the *full width at half maximum – FWHM*, which ultimately defines the spatial resolution. Although no single mathematical function can define those rough data, nor a *FWHM* for them either, an approximate evaluation for an equivalent parameter can be assigned to that first derivative.

Using this approach, that width agrees within 2 to 5% with the Gaussian FWHM depending on whether the maximum is measured from the right or from the left tail of the distribution.

III. EXPERIMENTAL

The experimental assembly to obtain the *Edge Response Function* and simultaneously the corresponding tomographic images is displayed in Fig. 6.

The *Argonauta* reactor at *Instituto de Engenharia Nuclear – CNEN Rio de Janeiro/Brazil* has been used as the source of thermal neutrons.

A bloc of paraffin fitted to the irradiation channel was used to thermalize the small fraction of epithermal neutrons. A 6cm-deep slit collimator cast in a lucite cylinder with its bases and internal walls lined with a 0.5mm-thick cadmium foil, was then introduced into that paraffin block whose free surface was also fully lined with a cadmium foil.

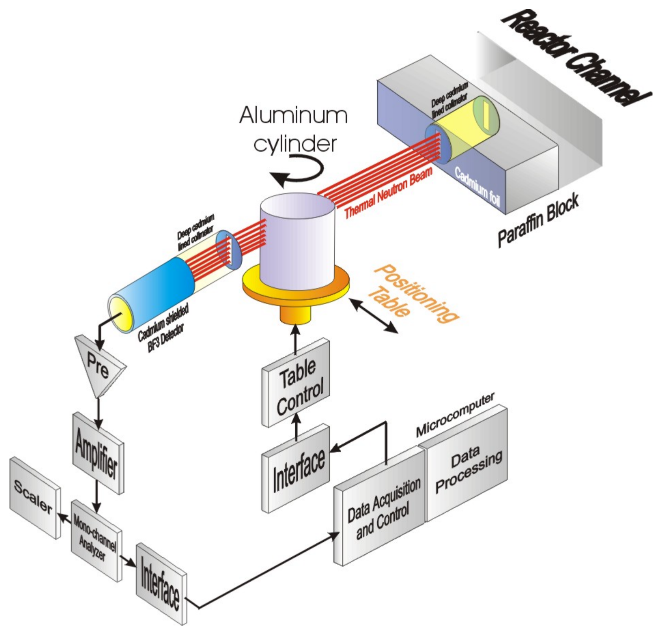

Figure 6. Experimental assembly used to determine the *Edge Response Function-ERF.* The collimator inside the paraffin block is aligned with that attached to the detector.

Another similar collimator was attached in front of a cadmium shielded BF_3 detector surrounded by a paraffin layer. It was aligned with the former one, assuring thus that the aluminum cylinder placed between the neutron source and the detector would be scanned by a parallel beam. That 50mm-diameter aluminum cylinder was fixed to a positioning table capable to translate and rotate in adjustable regular steps. After amplification, the pulses arising from the detector were discriminated, formatted by a monochannel analyzer and sent to a controller computer through a proper interface.

At each cycle generating one spectrum, i.e., one projection, the pulses were accumulated during a chosen time interval, in the 1^{st} channel of a computer-based multi-channel analyzer operating in the multi-scaler mode. The table then translated 1mm in a perpendicular direction to the neutron beam and the new counts were accumulated in the next channel of the MCA, until the completeness of a projection represented by a 66 channels spectrum.

After each spectrum, the table rotates by a chosen angle and returned to its initial position and started another cycle. The data acquisition and treatment as well as the control of the table movement was carried out using the software STAC5 developed at the *LIN-COPPE/UFRJ.* Further details can be found elsewhere [2].

IV. RESULTS AND DISCUSSION

Several ERF spectra required to obtain the LSF have been taken scanning an aluminum cylinder at 3 different angles of the positioning table, 0^0, 90^o and 180^o using slit collimators with the apertures of 1, 2, 3 and 5mm, all of them 10mm high. The spectra were not simply averaged as usually done, but instead of that, a function as given by equations (3-3a) with specific parameters T_0, D and w_{eff} have been fitted to each of them.

Parameter T_0 and an approximate value for D have been determined by fitting the Eq.(2) to the original ERF data while the effective collimator aperture has been picked up at the point where *S(m,k)* reaches its minimum value.

Each function was then numerically differentiated using a 0.1mm displacement step, rather than the original one (1.0mm) used for the experimental determination of the ERF. A Gaussian function was then fitted to the obtained derivatives and their FWHM plotted against the nominal collimator aperture actually used.

The average FWHM of these Gaussian curves associated to each collimator aperture actually used, are plotted in Fig.7 as bold blue triangles. For the sake of comparison, the raw experimental ERF spectra, have been also differentiated and Gaussian functions fitted to their *tails*. The individual results with the correspondent error bars and their averages are shown in Fig.7 as open and bold circles respectively.

The dependence of the LSF width - expressed by the FWHM of the associated Gaussian – with the nominal collimator aperture has been theoretically determined and is also shown in Fig. 7 as red triangles. The discrete points of this curve aren't free of uncertainty because the profile of the rough LSF as given by the discrete numerical differentiation of (3-3a) doesn't match perfectly the one of the Gaussian fitted to it. The width of both curves however, agrees within 2 to 5% with an ERF evaluated using 0.1mm displacement step.

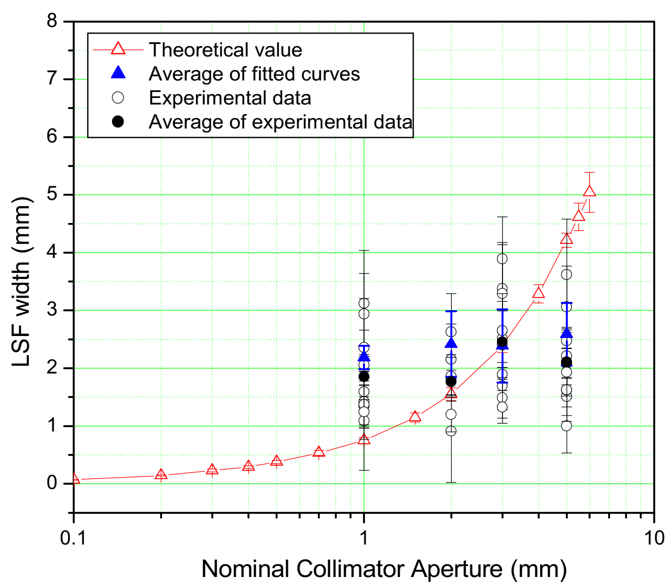

Figure 7. Dependence of the *Line Spread Function* width with the collimator aperture.

One can observe that the LSF widths deduced from the raw experimental data are much more spread than those arising from the fitted curves based on the collimator *effective aperture*. The average width of the last ones are affected by uncertainties larger than the theoretical values because the dispersion of the experimental data causes uncertainties in the effective aperture. The average values in both cases nevertheless agree within an error bar, showing a consistence between the results obtained by differentiation of the raw data and those obtained by the differentiation of the function fitted to them.

For both cases however, there's a substantial discrepancy between the theoretical LSF widths and those for 1 and 5mm-apertures. Although the error bars of the raw data overlap the theoretical curve, such a circumstance cannot be invoked as an argument for an even poor agreement, since the error bar associated to the average of the LSF width doesn't share this property. Neutron scattering could be a possible explanation for the large FWHM exhibited by the 1mm collimator.

The 5mm-aperture collimator exhibits a FWHM equivalent to an aperture of about 3mm. Such a reduction could be caused by alignment difficulties. Indeed, this alignment is a very difficult and cumbersome procedure due to the deep collimators utilized, their narrow slits and the large distance between them. Taking into account that each collimator has three degrees of freedom, any deviation from the correct alignment would diminish the effective aperture of the assembly.

All the data treatment has been performed by a Fortran computer program written for this purpose, aided by the non-linear fit option of the Microcal Origin 6.0 software.

REFERENCES

[1] ASTM E 1441-95 and 1570-95a, **Non-Destructive Testing, Radiation Methods, Computed Tomography, Guide for Imaging and Practice for Examination**, ISO/TC 135 / SC 5, N 118, 1996.

[2] Souza, M. I. S., **Tomografia computadorizada com nêutrons térmicos e detetor sensível à posição.** DSc. Thesis, COPPE/UFRJ 2001.